European Association for the
Development of Renewable Energies,
Environment and Power Quality (EA4EPQ)

International Conference on Renewable Energies and Power Quality
(ICREPQ'11)
Las Palmas de Gran Canaria (Spain), 13th to 15th April, 2011

Cell Method and Modified Nodal Method in Eddy Current Electromagnetic Problems

L. Simón and J.M. Monzón

Department of Electrical Engineering
University of Las Palmas de Gran Canaria
35017 – Tafira, Las Palmas (Spain)
Phone/Fax number:+0034 928 452888/451874, e-mail: **lsimon@pas.ulpgc.es**, **jmonzon@die.ulpgc.es**

Abstract. This paper present an approximation of an electromagnetic eddy current problem in 2D coupled with circuital equations, using the Finite Formulation of Electromagnetics Fields and the modified nodal method. The definition equations of the two conductor models (filiform and solid types) are deducted with this formulation. The analysis is performed at steady state and transient state. To the transient state, a classical scheme of time discretization is used with the implicit Runge-Kutta method for two states. As validation method have been compared results between Finite Element Method and Finite Formulation of Electromagnetics Fields.

Key words

Finite Formulation, Modified Nodal Method, Transient State, Implicit Euler Method.

1. Introduction

There are several references that use the circuital equations using modified nodal method (MNM) and finite element method (FEM) [1], [2], [3].
In this paper is used a variation of the modified nodal method (MNM) and the finite formulation of electromagnetics fields (FFEF) applied to the Maxwell's equations. With this procedure is possible to assemble the continuous behavior of the discretized field equations, with the circuital equations in a single matrix.

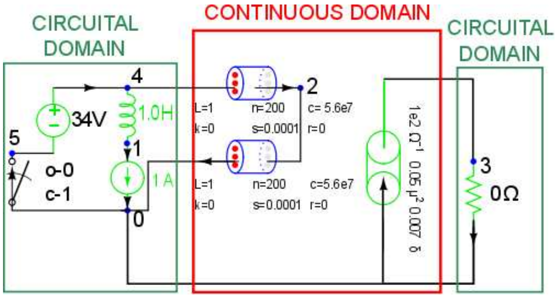

Fig. 1. Mixed-models representation.

The matrix equations are implemented with the Scilab, a scientific software package for numerical computations. To the continuous domain discretization is used the Gmsh program, that is an automatic 3D finite element mesh generator, with pre- and post-processing facilities [4].
In this paper is developed a method that uses both tools, the MNM and FFEF. This allows the simultaneous analysis of the distributed and concentrated models as shown in Fig. 1.

2. Finite Formulation

The finite formulation of electromagnetics fields (FFEF) is based on the use of scalar global variables [5], obtained by integrating field variables on a double system of meshes, strictly connected by relations of duality.
Global variables are distinguished in two types, the configuration variables (CV) associated to the primal mesh and the source variables (SV), associated to the dual one. CV involved in the magnetostatic problems are magnetic fluxes φ on primal faces and line integral *a* of magnetic vector potential on primal edges. The considered SV are magnetomotive forces *F* on dual edges.
The proposed solution relies on the portioning of the magnetic domain in a dual system of barycentric hexahedral meshes but the same theoretical scheme can be applied to unstructured meshes [6]. The topological magnetostatic equations are expressed according to Tonti formulation [5].

3. Variation of the MNM

The fundamental idea is to modify the MNM introducing two new sets respect to this method, so that the elements are separated into five disjoint sets between them Fig. 2.
In a first group A_1, those elements that can be expressed as admittances are included. In a second group A_2, are included those elements that can not be represented as admittance or a current value is required. The third group A_3, the independent current sources are included. In a fourth group A_4, the so called 'solid conductor model' elements are modeled. At this set are includes the voltages

and currents that are related with the FFEF and its numerical implementation with the cell method (CM), and finally the fifth group A_5, includes the filiform conductor model.
This is the key to eliminate all the circuital unknowns and to represent any linear element. This is not possible with the use of pure nodal methods or the mesh current method.

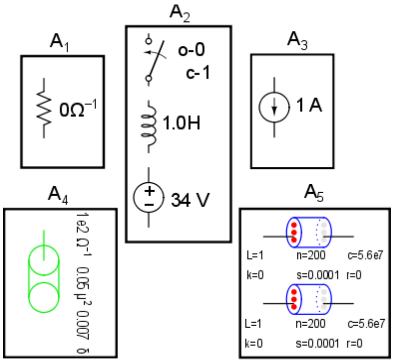

Fig. 2. The five set division.

We restructured the network elements so that the equations of the Kirchhoff's current law (KCL) can be written as,

$$\begin{bmatrix} A_1 & A_2 & A_3 & A_4 & A_5 \end{bmatrix} \cdot \begin{bmatrix} I_1 \\ I_2 \\ I_3 \\ I_4 \\ I_5 \end{bmatrix} \tag{1}$$

Being A_{nxbi} the circuital incidence matrix nodes-branches, where n is the number of nodes in the circuit minus 1 and b_i the number of elements of each one of the sets mentioned before.
The divisions are created so that:
The vector I_1 contains the currents through the branches of the elements that are represented in the form of admittance and that are not required as solutions.
Its defining equation is,

$$Y_1 \cdot U_1 = I_1 \tag{2}$$

Being Y_1 a diagonal matrix with dimension $[Y_1]_{b1xb1}$. The vector I_2 contains the currents through the branches of the elements that are not represented in the form of admittance. It also contains branch currents of voltage sources and currents of branches that are required as solutions. The equation defining these elements corresponds to the application of the Table Method (TM) and is

$$Y_2 U_2 + Z_2 I_2 = W_2 \tag{3}$$

where the second member W_2 only contains nonzero entries of the independent sources of tension, and the matrix Y_2 and Z_2 depend on the type of element.
The vector I_3 contains the independent current sources *(J)* $I_3 = J$.
The vector I_4 contains the current of the conductors at the continuous region with the solid conductor model.
The vector I_5 contains the conductors at the continuous region with the filiform conductor model.
The equations of the Kirchoff's voltage law (KVL) can be written in the same way.

$$\begin{bmatrix} U_1 \\ U_2 \\ U_3 \\ U_4 \\ U_5 \end{bmatrix} = \begin{bmatrix} A_1^T \\ A_2^T \\ A_3^T \\ A_4^T \\ A_5^T \end{bmatrix} \cdot V_n \tag{4}$$

Being $U_{i=1...5}$ vectors containing the potential differences of the elements at each set, and V_n a vector with the electric potential between each node and one reference node. The equations are represented in five individual matrix equations.

$$U_1 = A_1^T V_n \tag{5}$$

$$U_2 = A_2^T V_n \tag{6}$$

$$U_3 = A_3^T V_n \tag{7}$$

$$U_4 = A_4^T V_n \tag{8}$$

$$U_5 = A_5^T V_n \tag{9}$$

The equation (7) is used to determinate the voltage at the current sources once the V_n value has been determinated. Rewritting (1) as follows

$$A_1 I_1 + A_2 I_2 + A_4 I_4 + A_5 I_5 = -A_3 J \tag{10}$$

and substituting (2) in (10)

$$A_1 Y_1 U_1 + A_2 I_2 + A_4 I_4 + A_5 I_5 = -A_3 J \tag{11}$$

The voltages at the branches U_1 can be substituting by (5)

$$A_1 Y_1 A_1^T V_n + A_2 I_2 + A_4 I_4 + A_5 I_5 = -A_3 J \tag{12}$$

and in the same way substituting (6) in (3), we obtain

$$Y_2 A_2^T V_n + Z_2 I_2 = W_2 \tag{13}$$

The equations (12) and (13) will be used to complete in a single matrix equation all the unknowns.

4. Finite Formulation of the Maxwell's Equations

A. Topology of the Maxwell's Equations at Sinusoidal Steady

Consider two complexes dual meshes in R^3 called S and S'. For example, suppose that S is made of tetrahedra, and its volumes coincide with those tetrahedra. The set of dual mesh nodes S' contains an interior center point (barycentre of the tetrahedra) for each volume of the primal mesh, as shown Fig. 3.
Two nodes of the dual mesh complex S', are connected by straight segments passing through the barycenter of the triangular faces common to the primal mesh S.
This procedure establishes a bijective correspondence between the faces of the primal mesh and the edges of the dual mesh and vice versa, to each edge of the dual mesh there is a correspondence with one and only one face of the primal mesh [7], [8].
The quantities in Maxwell's equations are electrical voltage U, magnetic voltage F, electric flux Q, magnetic flux Φ and electric current I. These are defined by line

integrals and surface integrals of the basic field values as electric field strength $\vec{E}$,magnetic field strength $\vec{H}$,electric flux density $\vec{D}$,electric current density $\vec{J}$ and magnetic flux density $\vec{B}$.

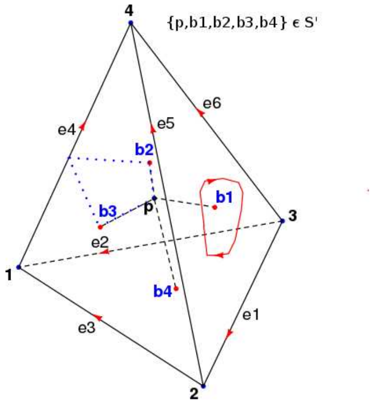

Fig. 3. Tetrahedra reference.

These integrals are assigned as unknowns to the elements of primal and dual meshes.
Topological equations of Maxwell's Laws to the magnetic field in sinusoidal steady [5]:
Gauss magnetic field theorem

$$D\phi = 0 \tag{14}$$

Faraday's law of induction

$$CU = -jW\phi \tag{15}$$

Developing the equation (15)

$$\sum_{j:e_j \in e} c_{i,j} u_j = -jW\phi_i, \forall i : f_i \in f \tag{16}$$

where the coefficients of the sum $c_{i,j} \in \{0, \pm 1\}$, i.e. for example, $c_{i,j} = \pm 1$ if $e_i \in \partial f_i$, where the signs correspond to the relative orientation of these elements, but if not then $c_{i,j}=0$.
Ampere's Law

$$\tilde{C}F = I \tag{17}$$

Law of continuity of current

$$\tilde{D}I = 0 \tag{18}$$

Being D_{vxf} the incidence matrix of pairs (v_i,f_j) of S, C_{fxe} the incidence matrix of pairs (f_i,e_j) of S and $\tilde{D}_{\tilde{v}\times\tilde{f}}$ the incidence matrix pairs $(\tilde{v}_i, \tilde{f}_j)$ of S' and $\tilde{C}_{\tilde{f}\times\tilde{e}}$ the matrix incidence of pairs $(\tilde{f}_i, \tilde{e}_j)$ of S'.
These matrix take into account the orientation of the identities involved. The faces of the S mesh and the corresponding dual edges have to be numbered and oriented consistently, i.e., $\tilde{G} = D^T$, $\tilde{C} = C^T$, $\tilde{D} = -G^T$, so that $DC=0$ and $\tilde{D}\tilde{C} = 0$. For 2D problems is verified $C = -G$ and $C^T = -G^T$. These relations are those for differential operators *div rot≡0*.

B. Constitutive Equations

The approach of the formulation is present when line and surface values are relationated with the meshes S and S' respectively.
The constitutive equations for (14), (18) are:

$$F = M_v\phi \tag{19}$$

$$I = M_\sigma U \tag{20}$$

The matrix M represent metric properties and medium properties, and a value transfer operator between S and S' (Hodge operator) [9]. The FFEF does not determine how to build this matrix. The way it is constructed is not unique and leads to different numerical schemes [5], [6].
The modeling in the FFEF is influenced by the generation of primal and dual meshes and the building materials constitutive equations, which include a average process of the properties of materials.

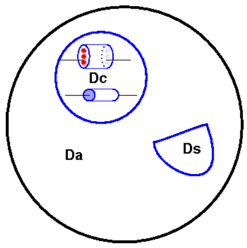

Fig. 4. Air, source and conductor domain set.

C. Solving Equations

As shows Fig. 4, if we know the current sources at D_s, the boundary conditions and initial conditions, then the solution of the problem search the unknowns $\{\Phi,U,F,I\}$.
To do this, the magnetic and electric potentials are used as auxiliary quantities. It makes problems easier and allow coupling the circuital and field equations easily.

D. Formulation {a, (a, V)}

The number of unknowns are reduced when working with the potentials a,V where $a = \int \vec{A}dl$ *(Weber)* is defined in the edges of the primal mesh e_i, and V *(Volts)* is the electric scalar potential related with the primal mesh nodes. If we define $\Phi=Ca$, Gauss's theorem is automatically satisfied if we do:

$$U = -jWa - GV \tag{21}$$

Faraday's Law is satisfied too, because is also true that $DG=0$, where G_{exn} is the incidence matrix between pairs (e_i,n_j). Substituting (19) in (17) we have $\forall e \in D_a \cup D_s$

$$\tilde{C}M_vCa = I \tag{22}$$

Substituting (20) in (22) and taking into account (21), we have $\forall e \in D_c$ that is true to the equation:

$$(\tilde{C}M_vC + jWM_\sigma)a + M_\sigma GV = 0 \tag{23}$$

Finally, substituting (21) in (20) and substituting (20) in (18), we have the continuity equation of the current $\forall n \in D_c$:

$$\tilde{D}M_\sigma(-jWa - GV) = 0 \tag{24}$$

5. Discretization of the Filiform Conductor Model (set type 5)

The equation of the filiform conductor model in 2D for an element, is obtained from a prismatic element with triangular base [10] as shown in Fig. 5.

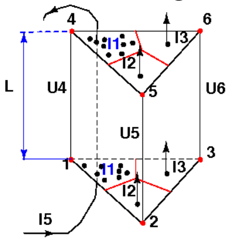

Fig. 5. Filiform conductor element.

This element will be crossed by a number of current filaments, as seen in Fig. 6.

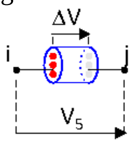

Fig. 6. Filiform conductor model.

If we have

$$\frac{\Delta}{3}[1 \quad 1 \quad 1]^T = [C_1]_e \tag{25}$$

and if we define $C_f^e = \left[N_f / \Omega_f\right][C_1]_e$, $\forall e \in \Omega_f$ and $\forall \Omega_f$ then:

$$+ jwC_f^T a - 1V_5 + R_f I_5 = 0 \tag{26}$$

Being $R_f = (N_f^2 L)/(\sigma \Omega_f)$ as a $b_5 x b_5$ diagonal matrix and C_f^T as a $b_5 xm$ matrix.

This equation relates global quantities from the purely circuital world (MNM) with global quantities associated to the side of the primal complex mesh (CM).

6. Discretization of the Solid Conductor Model (set type 4)

The global quantities [10] of the potential difference and current for a considered region in this model are showed in Fig. 7.

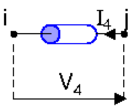

Fig. 7. Solid conductor model in a region.

Also Fig. 8 represents the solid conductor model for an element in a flat symmetric problem. To each region of the solid conductor model is defined $C_s = \sigma / L \times d_f \times C_1$ where $d_f = +1$ if the reference domain f is the same as the reference, and $d_f = -1$ if the direction of the domain f is contrary to the reference. If we consider more than one conducting region then I_4 and U_4 are grouped in $b_4 x1$ vectors and a $b_4 xn$ vector and the matrix Y_{b4xb4}. And we get the following equation:

$$- jwC_s^T a + Y_4 A_4^T V_n - I_4 = 0 \tag{27}$$

The relationship between the circuital world (MNM) and global quantities (CM) associated at the primal complex mesh is showed in this equation.

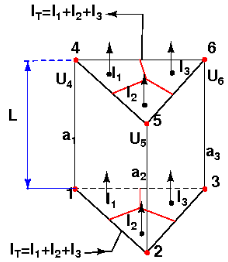

Fig. 8. Solid conductor model.

7. Ensemble of All Equations in a Global Matrix

As final results, the assemble of the continuous discretized field equations, with the circuital equations shown in a global matrix,

$$T = \begin{bmatrix} \tilde{C} M_\nu C + j\omega M_\sigma & -[C_s]A_4^T & 0 & 0 & -C_f \\ -j\omega C_s^T & Y_4 A_4^T & 0 & -1 & 0 \\ j\omega C_f^T & -A_5^T & 0 & 0 & R_f \\ 0 & A_1 Y_1 A_1^T & A_2 & A_4 & A_5 \\ 0 & Y_2 A_2^T & Z_2 & 0 & 0 \end{bmatrix} \tag{28}$$

The local definition of the terms is *column* x *bar number* and *column* x *node number*.

$$X = [a \quad V_n \quad I_2 \quad I_4 \quad I_5]^T \tag{29}$$

$$W = [0 \quad 0 \quad 0 \quad -A_3 J \quad W_2]^T \tag{30}$$

$$T \cdot X = W \tag{31}$$

Where respect to each set,

a , is the set of magnetic vector potential
V , are the nodal potential
I , are the independent currents sources
Z , impedances
Y , admittances
W , are the independent voltage sources
J , are current source from set 3
C , the curl matrix
$\tilde{C}$, the curl matrix at the dual
A , the incidence matrix
M_υ , the constitutive magnetic matrix
M_s , the constitutive conductivity matrix
R_f , winding resistance matrix

8. Solution in the time domain of the global formulation

The equation (31) can be resolved at the time domain and zero initial conditions (zero-state response) or with initial conditions that correspond to a steady state sinusoidal response (first and second Kirchoff's Law) [11].

The method divides the system matrix T in its real part G' and imaginary part C' ,

$$T = G' + iC' \quad (32)$$

Being *i* the imaginary unit, and given that each imaginary component corresponds to a temporal term of the form *d/dt*, the equation (31) has the form

$$G'X + C'\frac{dX}{dt} = W \quad (33)$$

then applied the Euler-Crank-Nicholson method we have the (34):

$$\left(\frac{C'}{\Delta t} + \theta \cdot G'\right) X^{n+1} = \left(\frac{C'}{\Delta t} - (1-\theta) G'\right) X^{n} + (1-\theta) W^{n} + \theta \cdot W^{n+1} \quad (34)$$

Where are different cases:
θ=1 Implicit Euler
θ=0 Explicit Euler
θ=0,5 Crank-Nicholson
θ=2/3 Galerkin

9. Results and discussion

The circuit scheme of example 1 shows in Fig. 9 consists of a current source of AC (element set type 3) and two conductive regions corresponding to a solid conductors models (elements set type 4) where all the elements are in series and connected as shown in Fig. 9.

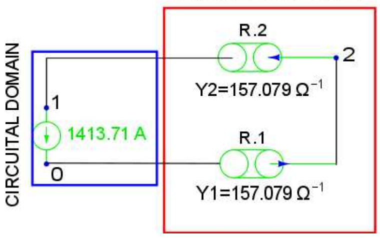

Fig. 9. Example 1 representing elements type 3 and type 4.

A section of the region known as discretized continuous domain is represented in Fig. 10. That is divided into five regions, the region number 1, correspond to the solid conductor between node 0 and node 2, see Fig. 10.

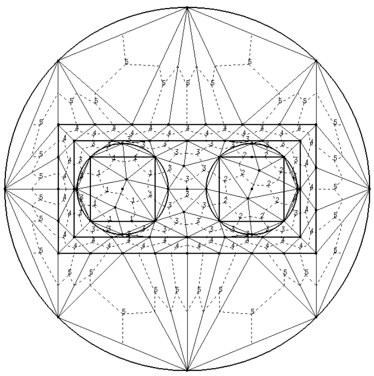

Fig. 10. Discretized continuous region in five parts of the primal and dual barycenter cell.

Region number 2 correspond to the solid conductor between node 2 and 1. The regions number 3, 4 and 5 in this problem corresponds to the air. As seen in Fig. 10 corresponds to the primal mesh triangles. At 3D would be a triangular base prisms. It is also noted the dual mesh, which corresponds to a barycentric division. For the matrix *T*, the matrices of equation (28) that are involved are

$$T = \begin{bmatrix} \tilde{C} M_v C + j\omega M_\sigma & -C_s A_4^T & 0 \\ -j\omega C_s^T & Y_4 A_4^T & -1 \\ 0 & 0 & A_4 \end{bmatrix} \quad (35)$$

and to the second member vector

$$W = \begin{bmatrix} 0 & 0 & -A_3 J \end{bmatrix}^T \quad (36)$$

the unknowns vector

$$\begin{bmatrix} a & V_n & I_4 \end{bmatrix}^T \quad (37)$$

At this example

$$A_4 = \begin{bmatrix} 0 & -1 \\ -1 & +1 \end{bmatrix} \quad (38)$$

$$A_3 = \begin{bmatrix} +1 & 0 \end{bmatrix}^T \quad (39)$$

$$J = [I] \quad (40)$$

$$Y_4 = \begin{bmatrix} \dfrac{\sigma^1 \Omega_1}{L} & 0 \\ 0 & \dfrac{\sigma^2 \Omega_2}{L} \end{bmatrix} \quad (41)$$

The data in Table I have been used for a number of experiences in sinusoidal steady state, and the results are summarized in Table II.

Table I.- Input parameters value

Magnitude	Value
I(A)	1413.7167
f(Hz)	50
Area1(m^2)	0.0001571
Area2(m^2)	0.0001571
L(m)	1
Y1(S) = Y2(S)	157.07963

In the Table II the results obtained by FEM are compared with those obtained by GetDP solver program [12], and shows the convergence of both results with the increasing number of nodes.

Table II.-Comparison of maximum induction value

Nodes	Elements	CM(Re)	FEM(Re)	CM(Im)	FEM(Im)
70	142	0.0607	0.0634	3.28e-5	3.32e-5
173	348	0.0517	0.512	5.11e-5	5.41e-5
507	1016	0.0528	0.0528	5.72e-5	5.82e-5
1096	2194	0.0537	0.0534	5.80e-5	5.94e-5

The potential difference results in the circuit are shown in Fig. 11, according to the second Kirchoff's Law. From the real and imaginary part of the magnetic induction, is deduced the total self induction coefficient of the equivalent circuit.
The continuous and discrete parameters models are shown in Fig. 12.

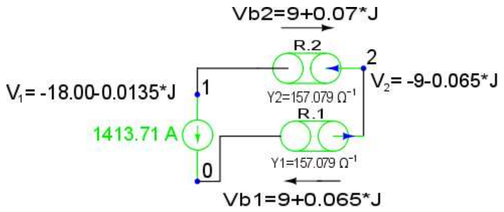

Fig. 11. Circuital results.

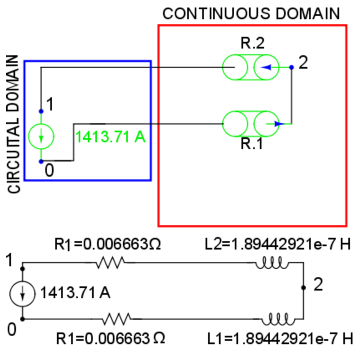

Fig. 12. Mixed model and pure lumped parameters.

Transient results for the solid conductor and the magnetic potential are represented in Fig. 13 and Fig. 14 respectively. Both results at the coordinate are shown in Fig. 14.

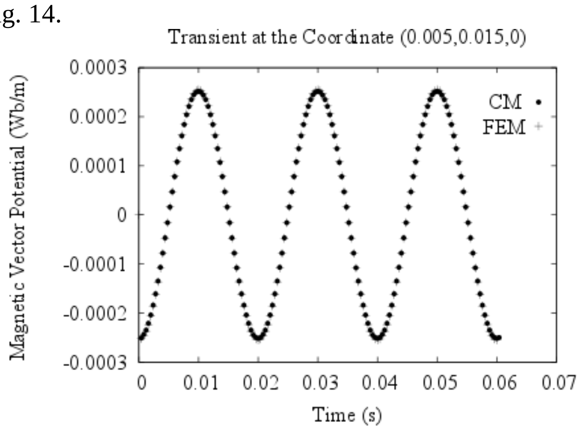

Fig. 14. Magnetic Vector Potential (for a length of m=1).

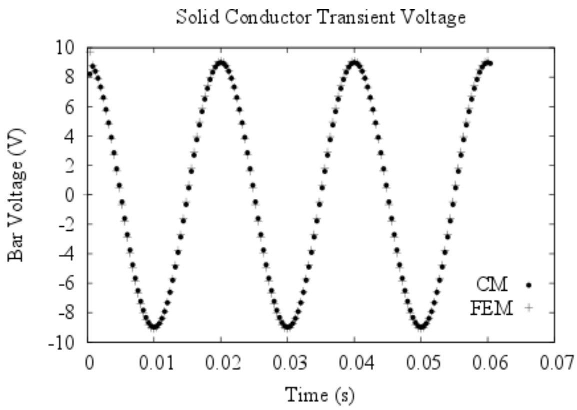

Fig. 13. Solid Conductor Voltage Transient.

Are also compared the results of the transient in the same time points with the results obtained of the GetDP program, which uses the finite element method.

10. Conclusions

We have presented an approximation of a 2D electromagnetic eddy current problem coupled with circuital equations, with the filiform conductor model and the solid conductor model. Study has been done using the Finite Formulation of Electromagnetics Fields and the Modified Nodal Method.

We have analyzed an example with the sets type 3 and type 4 elements. The results have been compared with two methods, the FEM and the FFEF. We have obtained the same results.

The analysis is performed at steady state and transient state.

To the transient state, a classical scheme of the Euler-Crank-Nicholson method for time discretization is used.

Acknowledgment

The authors gratefully acknowledge the support of the Department of Electrical Engineering of the University of Las Palmas de Gran Canaria, Spain.

References

[1] E. Strangas and K. Theis, “Shaded pole motor design and evaluation using coupled field and circuit equations,” Magnetics, IEEE Transactions on, vol. 21, pp. 1880–1882, Sep 1985.

[2] E. Strangas, “Coupling the circuit equations to the non-linear time dependent field solution in inverter driven induction motors,” Magnetics, IEEE Transactions on, vol. 21, pp. 2408–2411, Nov 1985.

[3] M. Costa, S. Nabeta, and J. Cardoso, “Modified nodal analysis applied to electric circuits coupled with fem in the simulation of a universal motor”, Magnetics, IEEE Transactions on, vol. 36, pp. 1431–1434, Jul 2000.

[4] C. Geuzaine and J. Remacle, “Gmsh: a three-dimensional finite element mesh generator with built-in pre-and post-processing facilities,” Int. J. for Numeric Method in Engineering, 2009.

[5] E. Tonti, “Finite formulation of electromagnetic field,” Magnetics, IEEE Transactions on, vol. 38, pp. 333-336, Ago 2002.

[6] M. Repetto, “3D magnetostatic with the finite formulation,” Magnetics, IEEE Transactions on, vol. 39, pp. 1135-1138, May 2003.

[7] M. Marrone, “Convergence and Stability of the Cell Method with Non Symmetric Constitutive Matrices,” COMPUMAG, no. 85, 2001.

[8] F. Trevisan and L. Kettunen, “Geometric interpretation of discrete approaches to solving magnetostatic problems,” Magnetics, IEEE Transactions on, vol. 40, pp. 361–365, March 2004.

[9] T. Tarhasaari, L. Kettunen, and A. Bossavit, “Some realizations of a discrete hodge operator: a reinterpretation of finite element techniques [for EM field analysis],” Magnetics, IEEE Transactions on, vol. 35, pp. 1494–1497, May 1999.

[10] W. Fu, P. Zhou, D. Lin, S. Stanton, and Z. Cendes, “Modeling of solid conductors in two-dimensional transient finite-element analysis and its application to electric machines,” Magnetics, IEEE Transactions on, vol. 40, pp. 426–434, March 2004.

[11] A. Nicolet and D. Delincé, “Implicit Runge-Kutta Methods for Transient Magnetic Field Computation” IEEE transactions on Magnetics, vol. 32, n. 3, 1996.

[12] P. Dular, C. Geuzaine, A. Genon, and W. Legros, “An evolutive software environment for teaching finite element methods in electromagnetism,” IEEE Transactions on Magnetics, vol. 35, pp. 1682–1685, May 1999.